RESEARCH PAPER

Liquid recirculation in microfluidic channels by the interplay of capillary and centrifugal forces

**Jose L. Garcia-Cordero · Lourdes Basabe-Desmonts ·
Jens Ducrée · Antonio J. Ricco**

Abstract We demonstrate a technique to recirculate liquids in a microfluidic channel by alternating predominance of centrifugal and capillary forces to rapidly bring the entire volume of a liquid sample to within one diffusion length, δ, of the surface, even for sample volumes hundreds of times the product of δ and the geometric device area. This is accomplished by repetitive, random sampling of an on-disc sample reservoir to form a thin fluid layer of thickness δ in a microchannel, maintaining contact for the diffusion time, then rapidly exchanging the fluid layer for a fresh aliquot by disc rotation and stoppage. With this technique, liquid volumes of microlitres to millilitres can be handled in many sizes of microfluidic channels, provided the channel wall with greatest surface area is hydrophilic. We present a theoretical model describing the balance of centrifugal and capillary forces in the device and validate the model experimentally.

Keywords Bio-sensors · Recirculation ·
Capillary forces · Centrifugal microfluidics ·
Surface tension · Diffusion

1 Introduction

Immunological assays such as ELISA (enzyme-linked immnosorbent assay) are among the most reliable and widely used techniques in medical diagnostics (Lai et al. 2004; Sia et al. 2004; Squires et al. 2008; Liu et al. 2009). Immunoassays are used to detect a variety of targets from raw samples: cells, bacteria, proteins, viruses, antigens, pollutants, hormones, peptides, nucleic acids and even pesticides (Delamarche et al. 2005). The combination of microfluidics with immunoassays, specifically with surface-bound probes, has demonstrated the potential to deliver low-cost, high-sensitivity, easy-to-operate, portable point-of-care (POC) devices (Sia et al. 2004).

In assays carried out using microfluidic architectures, target analytes can be delivered effectively to surface-immobilized receptors using less reagent volume and/or less time than bench-top counterparts (Hofmann et al. 2002). However, microfluidics has yet to become a work-horse for the analysis of precious raw samples containing very rare molecules or particles in large volumes, one important example being the detection of a handful of cancer cells in a few millilitres of whole blood (Nagrath et al. 2007), and another being the detection of certain proteins at femtomolar levels and below (one target molecule in a 100-μm cube) (Zheng et al. 2005). Recent advances show that some microfluidic systems can successfully tackle this problem, the price being laborious fabrication methods, expensive materials, and costly instrumentation (Zheng et al. 2005; Nagrath et al. 2007; Squires et al. 2008).

To improve limits of detection (LODs) in microfluidic devices in such instances, three approaches have been proposed: (1) using sensors (detectors) with exceptional limits of detection and specificity; (2) employing a reliable microfluidic strategy that delivers most of the analyte to the sensor very efficiently or (3) combining both approaches (Squires et al. 2008). Any approach must include consideration of time-to-result, as well as manufacturability

J. L. Garcia-Cordero · L. Basabe-Desmonts · J. Ducrée ·
A. J. Ricco (✉)
Biomedical Diagnostics Institute, National Centre for Sensor
Research, Dublin City University, Glasnevin, Dublin 9, Ireland
e-mail: ajricco@stanford.edu
URL: http://www.bdi.ie

issues, if it is to be considered for commercial point-of-care use.

Successful fluidic approaches to improve LODs require a major fraction of the target species in a liquid sample to have sufficient time to diffuse to the detection surface as the sample flows by. If this is not the case, larger sample volumes are needed to provide a given limit of detection with reasonable assay times. To avoid localized target depletion around the sensor area, quick replenishment with fresh sample is necessary, and this is often provided by high flow rates that further increase sample consumption (Parsa et al. 2008).

Several strategies have been proposed to efficiently deliver analyte to the sensing surface. The most obvious has been simple reduction of channel or chamber size, which may not necessarily accelerate target capture adequately to shorten assay times to a few minutes (Phillips et al. 2003) and can render some fluidic miniaturization strategies impractical. Reduction of channel height to dimensions where diffusion times are on the order of few seconds has been explored to increase sensor sensitivity (Hofmann et al. 2002; Phillips et al. 2003). However, reducing the channel dimensions implies either a reduction in volumetric flow rate and a corresponding increase in assay time, or an increase in pressure to often-impractical levels to maintain the same flow rates and assay times. In addition, channels with heights less than 20 μm are prone to clogging and remain challenging for large-scale manufacturing and bonding to other substrates.

Another strategy exploited in microfluidic devices is to flow the sample at very low flow rates (often nl/s) to provide enough time for analytes to diffuse to surface receptors (Parsa et al. 2008). However, for large sample volumes this approach may be impractical due to its adverse impact on assay time.

Another microfluidic strategy is to confine the sample using sheath flow to reduce the flow layer thickness of the original sample. Although this method reduced assay times from 55 to 13 min, it required 25 times more confining buffer than the original sample and relatively elaborate microfabrication techniques with exquisite flow control (Hofmann et al. 2002). Some groups have explored the use of continuously and discontinuously rotating chambers (Vanderhoeven et al. 2005), microfluidic planetary centrifugal mixing (Bynum and Gordon 2004), and electro-thermal stirring (Sigurdson et al. 2005).

On-chip passive mixing can also increase the rate of mass transfer to the sensor surface; this can be implemented by adding grooves, chevrons or other structures to microfluidic channel surfaces (Johnson et al. 2002; Stroock et al. 2002; Vijayendran et al. 2003; Nichols et al. 2006; Golden et al. 2007; Lee et al. 2009). Active mixing using external forces (El Moctar et al. 2003; Grumann et al. 2005; Ducree et al. 2006; Cho et al. 2007; Cao et al. 2008; den Toonder et al. 2008; Lynn et al. 2008; Wang et al. 2009) can also enhance the rate of mass transfer. However, these mixing strategies require precise flow control, can involve elaborate microfabrication techniques, or require coupling of external actuators to the microfluidic channel.

Relative to diffusion-limited mass transport, recirculation and other means of liquid movement can enhance capture efficiency for surface-binding or solution-phase reaction kinetics for a given interaction time by providing more (frequent) collisions of solution-phase species with one another or with binding sites (Abrantes et al. 2001; Chou et al. 2001; Yuen et al. 2003; Grumann et al. 2005; Lee et al. 2006; Liu et al. 2006). For a given assay time, (re)circulation can thus enable (i) use of smaller sample volumes without loss of assay sensitivity or (ii) more exhaustive sampling of larger sample volumes, improving limits of detection. Microfluidic recirculation has been shown variously to shorten nucleic acid hybridization times by 3×–10× compared to conventional methods (Yuen et al. 2003; Lee et al. 2006; Liu et al. 2006), to enhance reaction kinetics by almost two orders of magnitude (Chou et al. 2001), to reduce sample volume requirements by 1–3 orders of magnitude (Abrantes et al. 2001) and to accelerate mixing (Hosokawa et al. 1999; Handique and Burns 2001).

We report a technique to (re)circulate liquids through microfluidic channels in a compact disc (CD)-format fluidic device using the interplay of capillary and centrifugal forces, demonstrating that a liquid sample can be recirculated through a microchannel at least 1,000 times without observable change apart from slight evaporation (Garcia-Cordero et al. 2009). Li et al. (2009) have shown an important application of this approach to accelerating the rate of hybridization of DNA. We present here the physical equations and demonstrate the principles that govern this method, summarizing their implications for such key assay and device parameters as sample volume, channel volume, diffusion coefficient, channel height and number of 'spin cycles' required to achieve a given surface binding percentage of a low-concentration analyte.

Solely by manipulating disc spin rates and durations, a sample with many times the volume of the channel can be brought into surface contact in its entirety by introducing successive aliquots of the sample, removing each aliquot after a defined interaction time, re-mixing the entire sample, then introducing a fresh aliquot. Liquid volumes of microlitres to millilitres can be handled in many sizes of microfluidic channels, provided the channel wall with greatest surface area is hydrophilic.

Our approach is easily implemented compared to techniques requiring special microfabrication methods or syringe pumps (Abrantes et al. 2001; Chou et al. 2001; Yuen
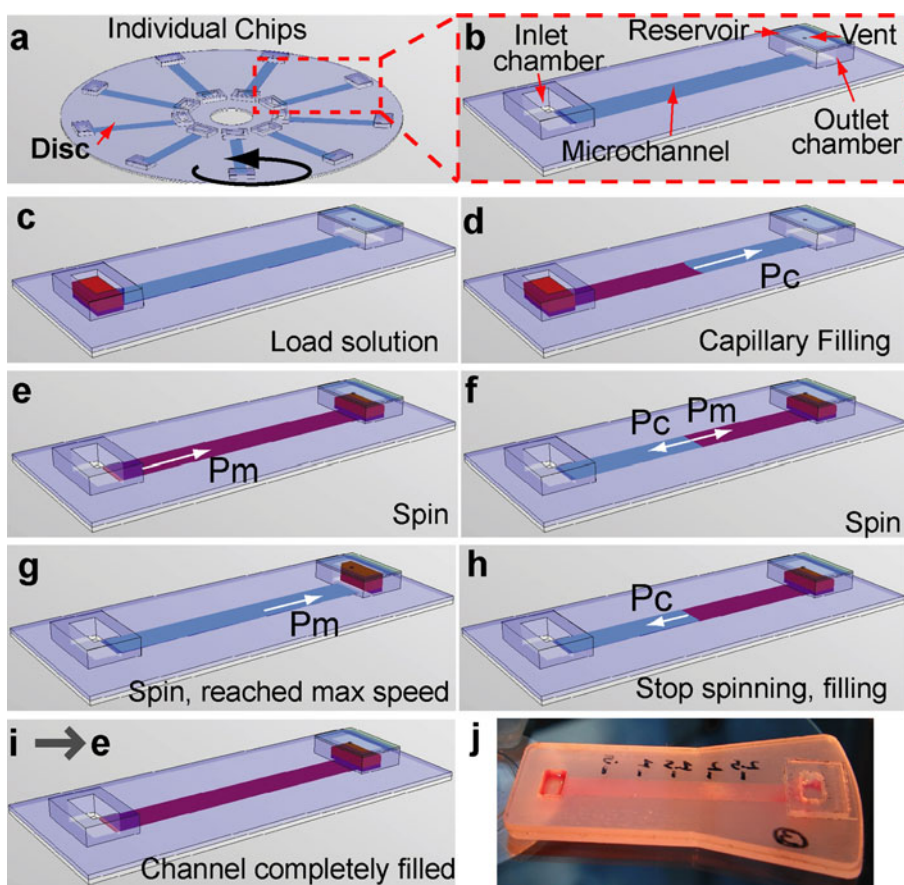
et al. 2003; Lee et al. 2006; Liu et al. 2006). The polymer-based devices are inexpensive to produce in quantity and easy to prototype: one hour from concept to completed device. Another advantage is that the equipment needed to drive this process is minimal, requiring only a low-cost motor to spin a compact disc (80 g weight) up to 1,500 rpm (CD player motors rotate at up to 3,000 rpm and are inexpensive: less than $US5 in electronics shops). Recirculation is achieved by spinning and stopping the disc.

2 Recirculation concept

The device and its conceptual operation, Fig. 1, show an inlet reservoir, a microfluidic channel, and a blind outlet reservoir that is vented by a small perforation to enable air ingress and egress. The top or bottom channel surface is hydrophilic to enable capillary filling. The inlet and outlet reservoirs, the volumes of which can exceed that of the solution to be circulated in a single cycle by many times, must be large enough to contain the entire sample volume. The connection to the outlet chamber is sufficiently narrow that liquid (re)fills the microchannel by capillary flow.

After the sample is introduced into the inlet reservoir, capillary action draws liquid into the channel. The fluid front stops at the junction between channel and outlet reservoir, leaving much or most of the liquid in the inlet reservoir. Spinning the device moves the fluid from the inlet, through the channel at a flow rate controlled by a combination of angular acceleration and final angular speed, into the outlet reservoir. This imparts momentum to the liquid moving from the channel into the outlet chamber, which exerts a force on the sample in the outlet reservoir. The centrifugal force also has a noticeable effect on the liquid contained in the outlet reservoir. At low angular speeds, the volume is spread uniformly over the entire 'floor' of the reservoir, but as speed increases and more sample volume is added to the outlet reservoir, the liquid is forced against the outer wall of the reservoir, the height of the liquid column then being limited by gravity and/or the top cover of the reservoir. The Coriolis pseudo-force can also help to mix at high angular speeds and for wide outlet reservoirs. The Coriolis effect forces the liquid to one side of the chamber during rotation (Brenner et al. 2005); that, combined with the fluid momentum, is another factor that changes the shape of the fluid within the reservoir in response to angular speed. Thus, two factors (driven by

Fig. 1 Process to (re)circulate liquids and capture scarce analytes. **a** A number of devices can fit on one CD. **b** Device schematic. Solution is loaded into the inlet reservoir (**c**), capillary forces draw liquid into the channel (**d**) until it reaches the outlet chamber, where it stops (**e**). Rotating the device forces the liquid to flow into the outlet reservoir (**f**, **g**). Immediately after stopping the device, liquid flows in the opposite direction (**h**), refilling the channel (**i**). This process is automatically repeated to sample the entire fluid volume (**i** → **e**). **j** Fabricated device

multiple phenomena), namely the momentum of the fluid entering the outlet reservoir and the changing shape and volume of the liquid in that reservoir, effectively mix the liquid by advection.

Once rotation stops, the now well-mixed liquid refills the channel by capillary action. This operation can be repeated many times, the mixing in the outlet chamber providing a random sample aliquot to the channel for each cycle.

3 Experimental details

3.1 Design of devices

Dimensions of microfluidic channels were 4 mm wide and 80 μm deep. The microfluidic channel length was 6 and 3.1 cm for the capillary filling and the centrifugal experiments, respectively. Devices were designed using a CAD program (AUTOCAD 2007, Autodesk, USA).

3.2 Fabrication of devices

Different materials were used for top and bottom channel surfaces: hydrophilic layers (MH90368, Adhesives Research, Ireland), poly(methylmethacrylate) (PMMA) sheets (Good-Fellow, UK), and cyclo-olefin polymer (COP) transparent compact discs (Zeonor 1060R, Zeon Chemicals, USA).

Devices were fabricated using multi-layer lamination as shown in Fig. 2 (Garcia-Cordero et al. 2009). A CO_2 laser system (Laser Micromachining LightDeck, Optec, Belgium) was used to cut the different plastic layers. Microfluidic channels were laser-cut from an 80-μm thick layer of double-sided pressure sensitive adhesive, d-PSA, film (AR9808, Adhesives Research, Ireland). Reservoir and inlet structures consisted of a 1-mm-thick layer of PMMA bonded to a d-PSA. The lid on the reservoir was made of a 0.2-mm-thick layer of PMMA bonded to a layer of d-PSA. A thermal roller laminator (Titan-110, GBC Films, USA) was employed to laminate the different polymer layers with the d-PSA films. For the assembly of all devices, the temperature in the laminator was set at 60°C with the distance between the rollers set to 1.5 mm.

The maximum length of a device is restricted to the axial length of the CD, which is 52.5 mm (inner radius 7.5 mm, outer radius 60 mm).

3.3 Test solution

To facilitate visualization of liquid displacement in the microchannels, a mixture of 40 ml of de-ionized water and 0.3 ml of red food coloring (Cochineal Artificial Food Colouring: Water, Colour (Carmoisine E122), Acid
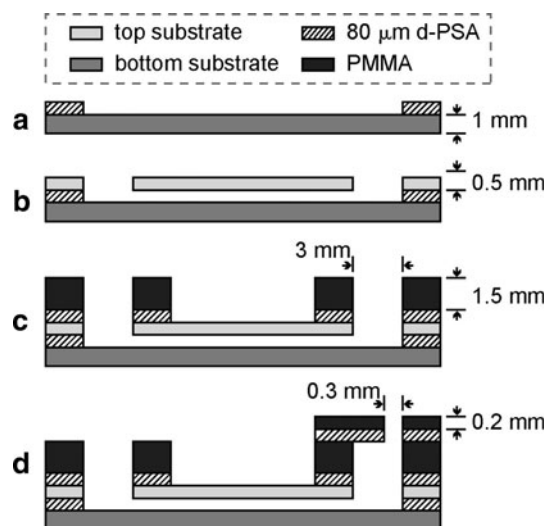

Fig. 2 Assembly of the recirculation microfluidic device. **a** The d-PSA is laminated to the bottom substrate. **b** The liner from the d-PSA is peeled off and the top substrate bonded onto it. The inlet and reservoir structures are created by **c** laminating a thick layer of acrylic with d-PSA onto the assembly. Finally, **d** a lid is attached to the reservoir structure using a thin layer of acrylic with d-PSA

(Acetic); Goodall's, Ireland) was used. Surface tension was assumed to be 71 dyn/cm, a density of 1 g/cm^3 and viscosity of 1 cP were also assumed, similar to the properties of water.

Contact angles of the different substrates were measured using a sessile drop analysis instrument (FTÅ200, First Ten Ångstroms, USA). Solution contact angles were measured as 12°, 76° and 90° for the hydrophilic layer, PMMA and COP, respectively.

3.4 Spinning station and optical setup

Fabricated devices were attached to a transparent compact disc (Åmic, Sweden). Discs were subsequently mounted on the spindle of a brushless DC motor with an integrated optical encoder (Series 4490, Faulhaber, Switzerland). Flow of liquids was monitored using a 12× motorized zoom lens (Navitar, UK) attached to a high-sensitivity camera (Sensicam QE, PCO AG, Germany). Motor and camera were controlled by a host computer. The motor triggered the camera every revolution to acquire images of the spinning disc. Camware (PCO AG, Germany) was used to acquire and analyze captured images.

4 Results and discussions

To control the movement of liquids in microchannels using this device, two types of force acting on the fluid must be taken into account: capillary and centrifugal. The capillary

force initially draws the liquid into the channel until it completely fills the channel. The filling speed is dictated by the hydrophilic properties (contact angle) of the channel's surfaces, its cross sectional area, and the fluid properties (viscosity, density, surface tension). When the disc is set in motion, the centrifugal force begins to displace the liquid in an outward direction from the centre of rotation; however, as any given section of the channel becomes empty, the capillary force continues to act in a manner that would refill the channel, essentially in opposition to the centrifugal force. Thus, the centrifugal force must exceed the capillary force (which is constant), a process enabled by sufficient rotational speed, as discussed in Sect. 4.2.

In this study, we studied and characterized the effect of both forces in microfluidic channels. Due to the small vertical dimension of the system, the effect of gravitational force is negligible, so it is not considered in these calculations.

4.1 Capillary filling

The interfacial pressure P_C of a liquid front advancing into a rectangular channel is given by (Delamarche et al. 2005; Parsa et al. 2008):

$$P_C = -\gamma \left(\frac{\cos \theta_B + \cos \theta_T}{h} + \frac{\cos \theta_L + \cos \theta_R}{w} \right) \quad (1)$$

where γ is the surface tension of the liquid, h and w are the height and width of the channel, respectively, and $\cos\theta_{B,T,L,R}$ are the contact angles of the liquid with the surface of the bottom, top, left and right walls, respectively.

To obtain the filling speed of a channel up to distance $L(t)$ by capillary action, the volumetric flow rate, Q, is given by

$$Q = \frac{\Delta P}{R} \quad (2)$$

subject to

$$Q = \frac{dV}{dt} = wh \frac{dL}{dt} \quad (3)$$

where $V(t)$ is the time-dependent volume filled, ΔP is the difference in pressure, and R is the hydrodynamic resistance of the channel, which for a rectangular microchannel for high-aspect ratio channels such that $w \gg h$ (our channels have an aspect ratio of 50:1) is given by (Bruus 2008):

$$R \approx \frac{12 \, \mu L}{wh^3} \left(1 - 0.63 \frac{h}{w} \right)^{-1} \quad (4)$$

where μ is the fluid viscosity. Substituting Eq. 4 in Eq. 2 and equating Eqs. 3 and 2, we arrive to the following:

$$L \cdot dL = P_C \frac{h^2(w - 0.63h)}{12\mu w} \cdot dt \quad (5)$$

Integrating Eq. 5 results in:

$$L(t) = \sqrt{P_C t \frac{h^2(w - 0.63h)}{6\mu w}} \quad (6)$$

which is also known as the Washburn equation (Washburn 1921) and describes the progression of the advancing meniscus in the microchannel at time t. Conversely, by expressing t as a function of L, Eq. 6 yields the (minimum) time required for the liquid to wick (back) into the channel.

In Fig. 3, experimental results are compared to theoretical values from Eq. 6. When at least one substrate is very hydrophilic (θ_B or $\theta_T < 15°$), filling times are independent of the contact angle of the opposing substrate and are significantly faster than when both substrates have identical, moderate contact angles ($\theta_B = \theta_T = 76°$).

Discrepancies between calculated and measured values may be attributable to the roughness of the channel side walls, which can 'pin' the fluid along the walls during filling, slowing the flow. Also, the Washburn equation neglects inertial effects, gravity, and deviations from a fully developed flow profile and a dynamic contact angle (Dreyer et al. 1994; Zhmud et al. 2000; Kusumaatmaja et al. 2008). Nonetheless, it can be concluded that when one substrate is highly hydrophilic, the difference between expected and measured fill time is typically less than 200 ms.
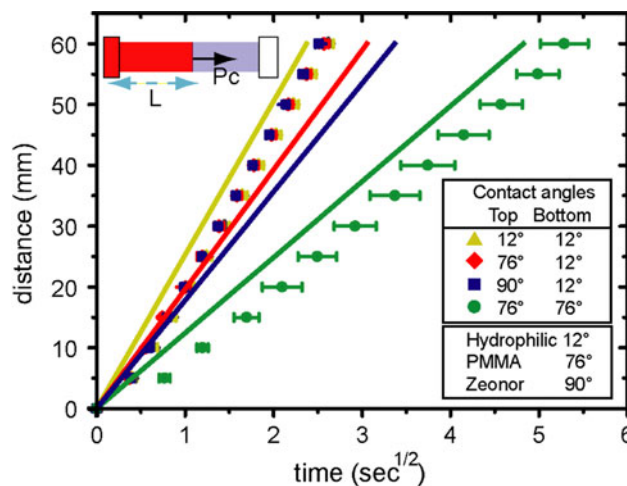

Fig. 3 Characterization of liquid filling an empty microchannel by capillary force as a function of the square root of time. Comparison of experimental (points are averages of 3 measurements) and theoretical values obtained from Eq. 6 (*lines*) for different top and bottom surface contact angles. Upper left schematic shows the capillary pressure, P_c, acting on the plug of liquid displaced by a distance L. The *error bars* represent the standard deviations from three independent measurements

4.2 Centrifugal–capillary interaction

The centrifugally induced hydrostatic pressure at the outer end of the liquid plug is given by (Duffy et al. 1999; Madou et al. 2006; Ducree et al. 2007):

$$P_m = \rho \omega^2 \bar{r} \Delta r \tag{7}$$

where ρ is the density of the liquid and ω is the angular velocity of the disc. We define

$$\bar{r} = (r_o + r_i)/2 \tag{8}$$

$$\Delta r = r_o - r_i \tag{9}$$

where $\bar{r}$ is the average distance of the liquid plug in the channel from the center of rotation and Δr is the radial length of the liquid plug as shown in Fig. 3. r_o and r_i are the inner and outer radii of the liquid plug, respectively.

r_o remains constant at all times because the liquid cannot go further than this point. Also, the capillary pressure is constant at the front end of the liquid plug. The maximum speed of rotation needed to displace the liquid from the inlet to the outer edge of the microfluidic channel, as well as the minimum speed needed for the liquid to return into the channel, can be calculated, as can the displacement distance of the liquid front, or r_i, at different angular speeds. The (stationary) equilibrium position, r_i, of the inner meniscus,

$$r_i = \sqrt{r_o^2 - \frac{P_C}{\rho \omega^2}} \tag{10}$$

occurs when P_m is equal to P_C at all times, with

$$P_C = \rho \omega^2 \left(r_o^2 - r_i^2 \right) \tag{11}$$

The liquid starts moving at an initial angular speed, ω_i, where the centrifugal pressure overcomes the capillary force, $P_m - P_C > 0$, thus

$$\omega_i > \sqrt{\frac{P_C}{\rho \left(r_o^2 - r_i^2 \right)}} \tag{12}$$

the final speed at which the liquid is fully displaced to the outlet chamber is

$$\omega_f > \sqrt{\frac{P_C}{\rho \left(r_o^2 - r_f^2 \right)}} \tag{13}$$

where r_f is the radius of the end of the microfluidic channel.

To verify these relationships, we fabricated three identical devices with lengths of 3.5 cm ($r_i = 2$ cm, $r_f = 5$ cm, $r_o = 5.5$ cm), widths of 4 mm and depths of 80 µm, using hydrophilic layers for top and bottom substrates ($\theta_B = \theta_T = 12°$). The total sample volume was 25 µl; the enclosed microchannel volume was ~11 µl. With these

values, Eq. 1 yields a capillary pressure of 1,214 Pa, from which Eq. 10 gives r_i as a function of ω, shown in Fig. 3; ω_i and ω_f were calculated from Eqs. 12 and 13 as 214 and 600 rpm, respectively.

Figure 4 shows that the liquid plug begins to move radially outward at 210 rpm, at which point centrifugal pressure overcomes capillary pressure. As ω increases, the liquid plug advances, reaching the channel end at 600 rpm. These values agree well with calculated results, 214 and 600 rpm.

4.3 Acceleration test

The flow velocity at which a solution passes over a capture region or sensor in a microchannel may affect the sensitivity and/or limit of detection of an assay or sensor. In some circumstances, it may be necessary to incubate the sample with the sensing surface region for a predetermined time, then replenish it with fresh sample solution. For example, a target protein in solution with a diffusion coefficient of 10^{-6} cm^2/s requires about 12 s to diffuse across a 50-µm channel; a red blood cell requires about 38 s to gravitationally sediment through that same distance. By selecting the angular acceleration, final angular velocity, and incubation time between successive 'spin cycles', this platform can adjust to the characteristic binding,
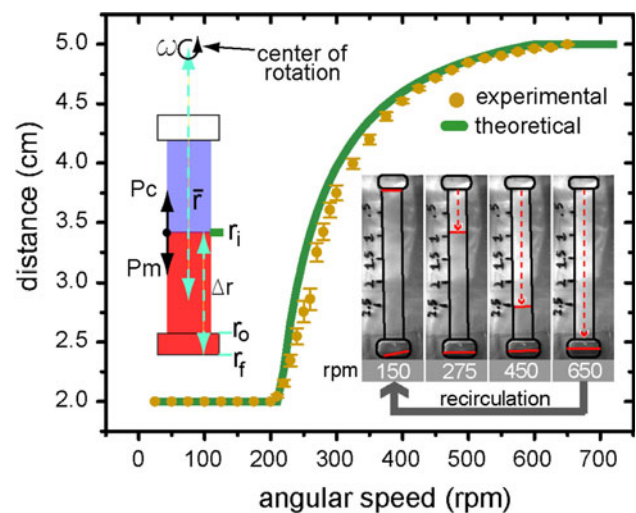

Fig. 4 Comparison of experimental and theoretical values for fluid radial displacement, r_i, versus the angular velocity ω of the disc. Sequence of images shows liquid displacement from the top (corresponding to the reservoir near the disc's center) at different angular speeds. The outlet chamber is marked by a *red bar* at the bottom of each image. If the angular speed is reduced below 200 rpm, liquid wicks back into the channel by capillary action. Left schematic shows the two forces acting on the plug of liquid and the dynamic radii. The *error bars* represent the standard deviation from five measurements

diffusion, and sedimentation times for any analyte and capture surface combination.

Using the device described above, a series of experiments revealed the time to flush the liquid from the microchannel into the outlet reservoir as a function of angular acceleration. For the range of accelerations and final frequencies studied, most of the liquid is displaced during the acceleration phase and is transferred to the outlet chamber by the time the final angular speed is attained, so the measurements were performed over a range of constant accelerations to the same final angular speed. The results, Fig. 5, show that evacuation time can be controlled from 5 s to 400 ms (a shorter channel, of course, would have shorter evacuation times). At low acceleration rates, it takes about 5 s to evacuate the liquid, whereas for acceleration rates above 4,000 rpm/s, this time remains below 500 ms. Reaching a high final angular speed rapidly via very high acceleration creates high centrifugal pressure that displaces the liquid to the outlet chamber in a very short period of time (average flow velocity: 60 mm/s). The minimum time to complete a cycle for this device would be 2.75 s (0.5 s to evacuate the channel, 2.25 s to refill it).

4.4 Sampling time

The recirculation concept can be exploited to capture analytes on a functionalized surface of the device, e.g., the bottom wall of the channel. Important considerations in the design of devices based on the recirculation concept are the dimensions of the channels (surface area to bind analytes and height of the channel, which plays a determining role in diffusion or sedimentation time) and the ratio of microchannel to total sample volume.
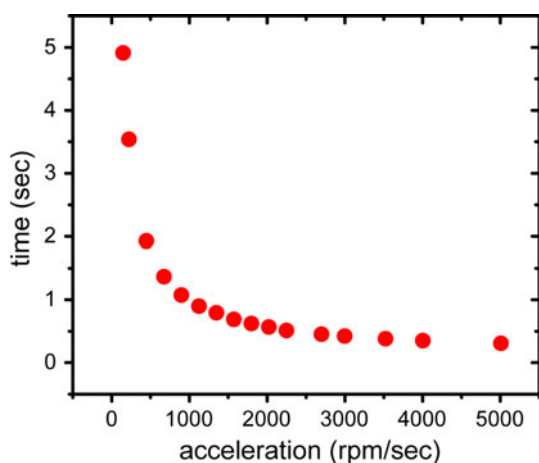

Fig. 5 Time to displace the liquid from the microchannel at different accelerations; in each case, acceleration continues until the microchannel is empty

The diffusion time for the target analyte (assuming the bottom surface of the channel is functionalized, and further assuming a molecular analyte, for which the rate of diffusion significantly exceeds the rate of gravitational sedimentation) will, in the first instance, dictate the height of the channel. In order to reduce the incubation time, the diffusion time for the target analyte to travel the height of the microchannel should be on the order of seconds.

The size of the sample volume versus the volume held by the microchannel is also a significant factor. For example, recirculating a volume in the millilitre range through a microfluidic channel in the microlitre range could take hours to sample completely. One possible solution to this problem is to divide the sample into multiple aliquots that are distributed into multiple microfluidic channels. This decreases the microchannel-to-sample volume ratio and thus reduces the number of cycles.

The particular details of the application will determine which factors can help to reduce the number of cycles and thus the time to result. Here, we introduce statistical calculations that help in choosing the appropriate device geometry in order to compute (and minimize) the number of cycles needed to capture a significant amount of the analyte.

For example, for respective sample and channel volumes of 100 and 25 μl, ideal mixing results in 25% 'sampling overlap' between two successive spin cycles; thus, statistically, a total of 16 cycles samples more than 99% of the fluid volume at least once. Similarly, a volume of 5 ml can be sampled in 15 μl aliquots with 95% efficiency by 1,000 successive cycles. The fraction, F, of the sample brought within one diffusion length of the surface (diffusion length being defined here as channel height) in n spin cycles is given by

$$F(n) = \sum_{i=1}^{n} p(1-p)^{i-1} \tag{14}$$

where p is the ratio of the microfluidic channel volume, V_M, to the total sample volume, V_T.

The probability of different fractions of sample volume-to-microchannel-volume ratios is plotted in Fig. 6. For a fraction 1/3, it takes 6 cycles to sample 90% of the volume, whereas it takes 45 cycles for a fraction of 1/50.

For the CD devices we fabricated, a surface area of 1 cm² is available for binding of analytes, so a 15-μl aliquot implies a channel height of 150 μm which, if defined to be the diffusion length, δ, yields a diffusion time of 113 s for an analyte with a typical diffusion coefficient of 10^{-6} cm²/s. With a total sample volume of 5 ml and 0.5 s allowed for each spinning step, this diffusion time implies a total assay time of 31 h for 1,000 spin cycles, an ineffective strategy for timely completion of an assay. Note,
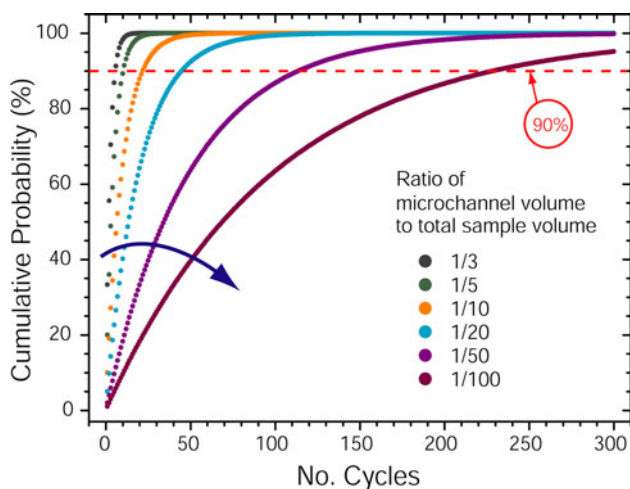
Fig. 6 Percentage of randomly distributed analyte molecules in a fluid sample brought within one diffusion length of the device surface as a function of the number of 'spin cycles' of a fluidic CD device. Calculated values from Eq. 14 are plotted for different ratios of microfluidic channel volume to total sample volume. For larger ratios (≥1/3), the sample volume is 90% sampled in less than 10 cycles, whereas for low ratios (≤1/50), over 100 cycles are needed to sample 90% of the sample volume

however, that if the assay detection limit goal can be attained by 50% sampling, only 231 cycles are required; further, if the assay surface area is increased to 6 cm^2 and the channel height decreased to 25 μm (readily accessible with the CD format and using off-the-shelf PSA films), assay time per spin cycle is 3.1 s and overall assay time for 50% sampling is just 14 min. Thus, an informed design of device geometry and assay process can produce a useful assay result some 130 times more quickly than the uninformed approach.

5 Design rules

To design new devices based on this technique, we suggest these rules:

1. Define total sample volume and microfluidic channel volume. Design and fabricate outlet and inlet chambers as well as microfluidic channel accordingly.
2. Obtain the surface tension and contact angle of solutions with surface.
3. Get the dimensions of microfluidic channel and the radius of the end of the microfluidic channel.
4. Obtain the capillary pressure using Eq. 1.
5. Calculate the minimum filling time of channel if needed using Eq. 6.
6. Minimum and maximum angular speeds can be calculated from Eq. 12 and 13.
7. If need be, approximate flow velocity can be calculated based on the angular acceleration.

8. Use Eq. 14 to estimate the minimum number of cycles that device has to be spun to statistically sample the full volume

6 Conclusions

In summary, we have presented results from, as well as the fundamental physical principals underlying, a new technique to recirculate large-volume samples in microfluidic channels using a rotational platform. The interplay of capillary and centripetal forces makes it possible to move liquid repetitively through the channel, bringing a freshly mixed sample aliquot into the channel with each cycle. We provide a theoretical framework with which to calculate the speeds of rotation needed to circulate the liquid, facilitating the design of new devices that use this technique. We also presented results for, and compared with calculations, the time to fill a microfluidic channel for varying surface properties.

References

Abrantes M, Magone MT, Boyd LF, Schuck P (2001) Adaptation of a surface plasmon resonance biosensor with miorofluidics for use with small sample volumes and long contact times. Anal Chem 73(13):2828–2835

Brenner T, Glatzel T, Zengerle R, Ducree J (2005) Frequency-dependent transversal flow control in centrifugal microfluidics. Lab Chip 5(2):146–150

Bruus H (2008) Theoretical microfluidics. Oxford University Press, USA

Bynum MA, Gordon GB (2004) Hybridization enhancement using microfluidic planetary centrifugal mixing. Anal Chem 76(23):7039–7044

Cao J, Cheng P, Hong FJ (2008) A numerical study of an electrothermal vortex enhanced micromixer. Microfluid Nanofluid 5(1):13–21

Cho YK, Lee JG, Park JM, Lee BS, Lee Y, Ko C (2007) One-step pathogen specific DNA extraction from whole blood on a centrifugal microfluidic device. Lab Chip 7(5):565–573

Chou H-P, Unger MA, Quake SR (2001) A microfabricated rotary pump. Biomed Microdevices 3(4):323–330

Delamarche E, Juncker D, Schmid H (2005) Microfluidics for processing surfaces and miniaturizing biological assays. Adv Mater 17(24):2911–2933

den Toonder J, Bos F, Broer D, Filippini L, Gillies M, de Goede J, Mol T, Reijme M, Talen W, Wilderbeek H, Khatavkar V, Anderson P (2008) Artificial cilia for active micro-fluidic mixing. Lab Chip 8(4):533–541

Dreyer M, Delgado A, Rath HJ (1994) Capillary rise of liquid between parallel plates under microgravity. J Colloid Interface Sci 163(1):158–168

Ducree J, Brenner T, Haeberle S, Glatzel T, Zengerle R (2006) Multilamination of flows in planar networks of rotating micro-channels. Microfluid Nanofluid 2(1):78–84

Ducree J, Haeberle S, Lutz S, Pausch S, von Stetten F, Zengerle R (2007) The centrifugal microfluidic bio-disk platform. J Micromech Microeng 17(7):S103–S115

Duffy DC, Gillis HL, Lin J, Sheppard NF, Kellogg GJ (1999) Microfabricated centrifugal microfluidic systems: characterization and multiple enzymatic assays. Anal Chem 71(20):4669–4678

El Moctar AO, Aubry N, Batton J (2003) Electro-hydrodynamic micro-fluidic mixer. Lab Chip 3(4):273–280

Garcia-Cordero JL, Basabe-Desmonts L, Ducree J, Lee LP, Ricco AJ (2009) Liquid recirculation in microfluidic channels by the interplay of capillary and centrifugal forces. The 15th international conference on solid-state sensors, actuators, and microsystems. IEEE, USA

Golden JP, Floyd-Smith TM, Mott DR, Ligler FS (2007) Target delivery in a microfluidic immunosensor. Biosens Bioelectron 22(11):2763–2767

Grumann M, Geipel A, Riegger L, Zengerle R, Ducree J (2005) Batch-mode mixing on centrifugal microfluidic platforms. Lab Chip 5(5):560–565

Handique K, Burns MA (2001) Mathematical modeling of drop mixing in a slit-type microchannel. J Micromech Microeng 11(5):548–554

Hofmann O, Voirin G, Niedermann P, Manz A (2002) Three-dimensional microfluidic confinement for efficient sample delivery to biosensor surfaces. Application to immunoassays on planar optical waveguides. Anal Chem 74(20):5243–5250

Hosokawa K, Fujii T, Endo I (1999) Handling of picoliter liquid samples in a poly(dimethylsiloxane)-based microfluidic device. Anal Chem 71(20):4781–4785

Johnson TJ, Ross D, Locascio LE (2002) Rapid microfluidic mixing. Anal Chem 74(1):45–51

Kusumaatmaja H, Pooley CM, Girardo S, Pisignano D, Yeomans JM (2008) Capillary filling in patterned channels. Phys Rev E 77(6):067301

Lai S, Wang SN, Luo J, Lee LJ, Yang ST, Madou MJ (2004) Design of a compact disk-like microfluidic platform for enzyme-linked immunosorbent assay. Anal Chem 76(7):1832–1837

Lee HH, Smoot J, McMurray Z, Stahl DA, Yager P (2006) Recirculating flow accelerates DNA microarray hybridization in a microfluidic device. Lab Chip 6(9):1163–1170

Lee MG, Choi S, Park JK (2009) Rapid laminating mixer using a contraction–expansion array microchannel. Appl Phys Lett 95(5):1–051902

Li CY, Dong XL, Qin JH, Lin BC (2009) Rapid nanoliter DNA hybridization based on reciprocating flow on a compact disk microfluidic device. Anal Chim Acta 640(1–2):93–99

Liu J, Williams BA, Gwirtz RM, Wold BJ, Quake S (2006) Enhanced signals and fast nucleic acid hybridization by microfluidic chaotic mixing. Angew Chem Int Ed 45(22):3618–3623

Liu CC, Qiu XB, Ongagna S, Chen DF, Chen ZY, Abrams WR, Malamud D, Corstjens PLAM, Bau HH (2009) A timer-actuated immunoassay cassette for detecting molecular markers in oral fluids. Lab Chip 9(6):768–776

Lynn NS, Henry CS, Dandy DS (2008) Microfluidic mixing via transverse electrokinetic effects in a planar microchannel. Microfluid Nanofluid 5(4):493–505

Madou M, Zoval J, Jia GY, Kido H, Kim J, Kim N (2006) Lab on a CD. Annu Rev Biomed Eng 8:601–628

Nagrath S, Sequist LV, Maheswaran S, Bell DW, Irimia D, Ulkus L, Smith MR, Kwak EL, Digumarthy S, Muzikansky A, Ryan P, Balis UJ, Tompkins RG, Haber DA, Toner M (2007) Isolation of rare circulating tumour cells in cancer patients by microchip technology. Nature 450(7173):U10–U1235

Nichols KP, Ferullo JR, Baeumner AJ (2006) Recirculating, passive micromixer with a novel sawtooth structure. Lab Chip 6(2):242–246

Parsa H, Chin CD, Mongkolwisetwara P, Lee BW, Wang JJ, Sia SK (2008) Effect of volume- and time-based constraints on capture of analytes in microfluidic heterogeneous immunoassays. Lab Chip 8(12):2062–2070

Phillips C, Jakusch M, Steiner H, Mizaikoff B, Fedorov AG (2003) Model-based optimal design of polymer-coated chemical sensors. Anal Chem 75(5):1106–1115

Sia SK, Linder V, Parviz BA, Siegel A, Whitesides GM (2004) An integrated approach to a portable and low-cost immunoassay for resource-poor settings. Angew Chem Int Ed 43(4):498–502

Sigurdson M, Wang DZ, Meinhart CD (2005) Electrothermal stirring for heterogeneous immunoassays. Lab Chip 5(12):1366–1373

Squires TM, Messinger RJ, Manalis SR (2008) Making it stick: convection, reaction and diffusion in surface-based biosensors. Nat Biotechnol 26(4):417–426

Stroock AD, Dertinger SKW, Ajdari A, Mezic I, Stone HA, Whitesides GM (2002) Chaotic mixer for microchannels. Science 295(5555):647–651

Vanderhoeven J, Pappaert K, Dutta B, Van Hummelen P, Desmet G (2005) DNA microarray enhancement using a continuously and discontinuously rotating microchamber. Anal Chem 77(14):4474–4480

Vijayendran RA, Motsegood KM, Beebe DJ, Leckband DE (2003) Evaluation of a three-dimensional micromixer in a surface-based biosensor. Langmuir 19(5):1824–1828

Wang SS, Jiao ZJ, Huang XY, Yang C, Nguyen NT (2009) Acoustically induced bubbles in a microfluidic channel for mixing enhancement. Microfluid Nanofluid 6(6):847–852

Washburn EW (1921) The dynamics of capillary flow. Phys Rev 17(3):273

Yuen PK, Li GS, Bao YJ, Muller UR (2003) Microfluidic devices for fluidic circulation and mixing improve hybridization signal intensity on DNA arrays. Lab Chip 3(1):46–50

Zheng GF, Patolsky F, Cui Y, Wang WU, Lieber CM (2005) Multiplexed electrical detection of cancer markers with nanowire sensor arrays. Nat Biotechnol 23(10):1294–1301

Zhmud BV, Tiberg F, Hallstensson K (2000) Dynamics of capillary rise. J Colloid Interface Sci 228(2):263–269